VALIDATION OF THE MEWA CODE AGSINST POMECO-HT EXPERIMENTS AND COOLABILITY ANALYSIS OF STRATIFIED DEBRIS BEDS

Zheng Huang, Weimin Ma, Sachin Thakre
Royal Institute of Technology (KTH), Stockholm, Sweden
hzheng@kth.se, weimin@kth.se, thakre@safety.sci.kth.se

ABSTRACT

Motivated by qualification of the MEWA code for coolability analysis of debris beds formed during severe accidents of light water reactors, the present work presents a validation of the code against the experimental data obtained on the POMECO-HT facility for investigation of two-phase flow and heat transfer limits in particulate beds with various characteristics. The volumetrically heated particulate beds used in the POMECO-HT experiment are packed in various configurations, including homogeneous bed, radially stratification, triangular stratification, axial stratification, and multi-stratification. To investigate coolability enhancement by bottom-fed induced natural circulation, a downcomer is employed. Besides, the influence of the interfacial drag is also studied. The results show that simulation results of the MEWA code is overall comparable with the experimental data in term of dryout conditions of the particulate beds. For the 1-D top-flood case, the dryout heat flux is mainly determined by counter-current flow limit. While for certain cases the multidimensionality may help to break CCFL. Besides, the debris bed's coolabiltiy can be significantly improved due to the natural circulation flow from the bottom induced by using downcomer. The interfacial drag affects the coolability by means of varying the pressure field inside the bed. For the top-flood case, the dryout condition deteriorates since the vapor and coolant flow reversely and thus the interfacial drag increases the flow resistance. Whereas for the bottom-fed case, the dryout heat flux rises remarkably when considering the interfacial drag, because the vapor and coolant flow in the same direction and the interfacial drag helps to pull coolant upward from the bottom.

KEYWORDS
Severe accident; Debris bed; Coolability; MEWA code simulation; Interfacial drag

1. INTRODUCTION

During a severe accident of a nuclear power plant (NPP), the molten core materials may relocate either in the lower head of reactor vessel (in-vessel) or in the reactor cavity (ex-vessel), and contact the coolant, resulting in rapid quenching and fragmentation. Subsequently, the particulate corium may settle down on available surfaces, forming a porous debris bed. To terminate and stabilize the accident progression, the debris bed need continuous cooling because of the decay heat generated within it. On the other hand, the debris bed is easier to be cooled than the molten corium pool since the porous nature of the bed is more accessible for coolant to penetrate through the pores of the bed and remove the internal heat by evaporation. In this process, the dryout heat flux (DHF), i.e. the maximum heat flux that can be removed from the bed without incipient dryout, is considered as the limiting criterion to assess the coolability of the debris bed. Therefore, the assessment of the coolability of debris bed and the prediction of DHF are paramount to the severe accident management strategy and safety margin evaluation.

A number of experimental investigations have been carried out to study the two-phase flow through the porous medium and heat transfer phenomenon [1-3]. And numerous analytical model and empirical correlations were developed to predict the two-phase flow pressure drop and DHF in particulate bed [4-7]. From the literature survey it is found that most of the previous studies are primarily focused on the homogeneous and one-dimension cylindrical configuration with coolant flooding from the top, in which case the DHF depends on the Counter-Current Flow Limit (CCFL). However, in realistic accident scenarios, the debris bed may not spread uniformly. One of the most important bed geometry may be heap-like (conical) or mound-like, characterized by the lateral or bottom ingression of coolant [8]. Such multi-dimensionality of debris bed tends to increase the DHF and enhance the coolability [2, 9].

In order to describe the transient boil-off and quenching behaviors of debris bed, MEWA code was developed by IKE-Stuttgart University in the frame of the KESS code system, aiming at assessment of debris bed [10]. Motivated by qualification of the MEWA code and better understanding the effect of stratified configuration of debris bed on its coolability, the present work presents a validation of the code against the experimental database obtained from the POMECO-HT facility. Afterwards, the assessment of the coolability of prototypical-scale debris featuring the similar characteristics is performed.

2. POMECO-HT EXPERIMENTS

2.1. Test Facility

In order to study the effect of various characteristics of debris bed on coolability, a series of experiments mainly focusing on the DHF were conducted on the POMECO-HT facility at Royal Institute of Technology (KTH) [11,12]. The test facility features a high heat flux up to 2.1 MW/m^2 enabling wide range of debris bed configuration to reach dryout condition. As shown in Fig. 1, the facility consists of test section, water supply system, electrical heaters, downcomer (DC) and data acquisition system (DAS).

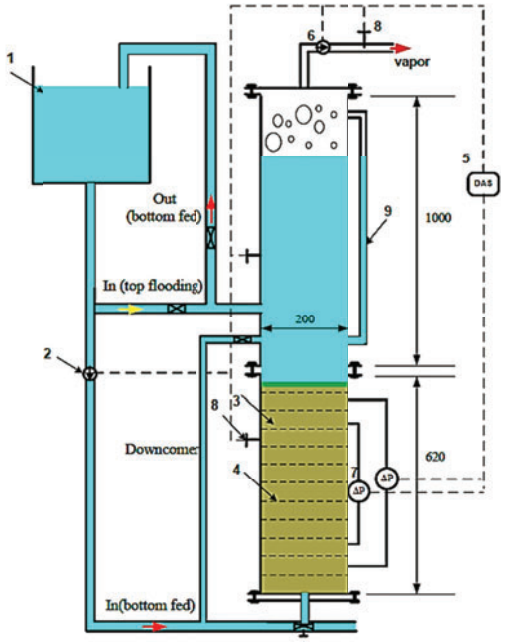

1-water tank, 2-water flowmeter, 3-particle bed, 4-heaters, 5-data acquisition system, 6-steam flowmeter, 7-pressure transducer, 8-thermocouples, 9-water level gauge

Figure 1. Schematic Diagram of POMECO-HT Facility

The tests section accommodating the particulate bed and heaters is a stainless steel vessel with the rectangular cross-sectional area of 200mm×200mm and the height of 620mm. Above the test section sits a stainless steel water tank (200mm×200mm×1000 mm) connected to the test section through flanges. The test section and the water tank are well insulated. A total number of 120 electrical resistance heaters are uniformly distributed in the particulate bed in 15 vertical layers (cf. Fig. 2). The power rating of each heater is 700W, so the maximum power capacity of facility is 84kW. The particulate bed is also equipped with 96 thermocouples installed at 16 vertical levels, with 6 thermocouples at each plane. The diameter of each thermocouple is 1.5 mm with various lengths inserted in the bed. Each heater has the diameter of 3 mm and the total length of 235 mm, with the heated part of 195 mm. So the heaters and thermocouples occupy about 0.7% in volume of the test section.

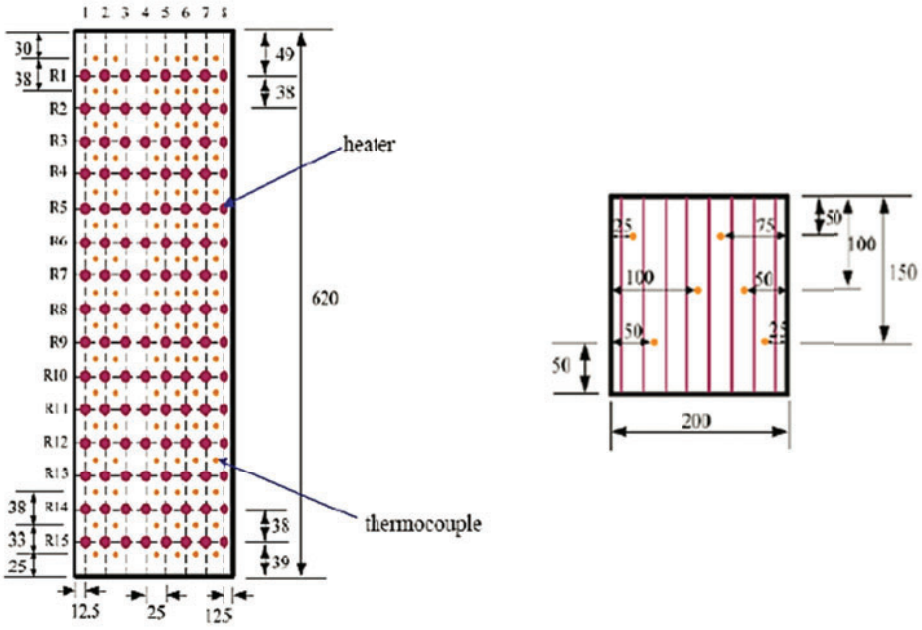

(a) side view (b) top view

Figure 2. Distribution of Heaters and Thermocouples

2.2. Test Particulate Beds

Six test particulate beds, regarding different particle diameter and porosity distribution, are selected in the present work. The Configuration and the detail parameters of each bed can be seen in Fig. 3 and Table I.

The cross section of all the test beds is rectangular with the area being 200mm×200mm. The height of the first four beds is 610mm, while for Bed-4 and Bed-5, the height is shorter (362mm). Bed-1 and Bed-2 are both homogeneous beds, packed with stainless steel spheres of 1.5 and 3.0 diameter respectively. Bed-3 is radially stratified. The middle column filling with the 1.5mm particles is 100mm in width, with the porosity of 0.363, whereas the rest part at each side is filled with the 3.0mm particles with larger porosity (0.367). The triangular bed (Bed-4) is similar to Bed-3, except that the cross section of middle part is in a shape of isosceles triangle in vertical direction while rectangle from the top view. It should be noted that only the triangular part is heated during experiment, while the electrical resistance heaters in the rest part are disconnected from the power source. Bed-5 is horizontally divided into two equal parts. The upper part is filled with smaller particle (1.5mm) with porosity of 0.387, whereas the lower part is packed with 3.0mm spheres with porosity of 0.393. Beds-6, featuring multidimensional stratification, is divided into

four equal zones. The lower right and upper left parts (zone1 and zone3) are filled with single-size particles (1.5mm and 3.0mm in diameter respectively), whereas the particles in the rest parts (zone2 and zone4) are the mixture of these two-size stainless steel spheres.

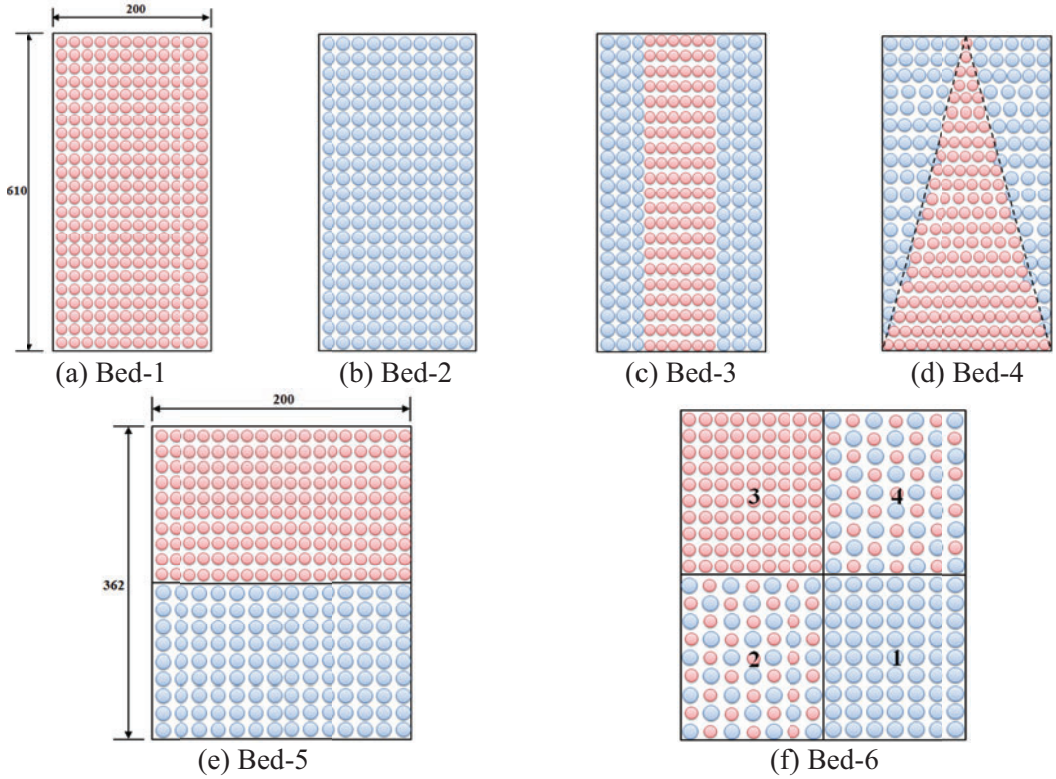

Figure 3. Configuration of Various Test Debris Beds

Table I. Details of Particulate Bed Parameters

Bed	Type of bed	Particle diameter (mm)	Porosity (-)	Bed height (mm)
Bed-1	Homogeneous	1.5	0.363	610
Bed-2	Homogeneous	3.0	0.367	610
Bed-3	Radially stratified	Inner: 1.5 Outer: 3.0	Inner: 0.363 Outer: 0.367	610
Bed-4	Triangular	Inner: 1.5 Outer: 3.0	Inner: 0.363 Outer: 0.367	610
Bed-5	Horizontally stratified	Upper:1.5 Lower: 3.0	Upper: 0.387 Lower: 0.393	362
Bed-6	Multiply stratified	Zone 1: 3.0 Zone 2: 1.5 and 3.0 Zone 3: 1.5 Zone 4: 1.5 and 3.0	Zone 1: 0.398 Zone 2: 0.406 Zone 3: 0.439 Zone 4: 0.366	362

3. MEWA CODE MODEL

The MAWA code (previously called WABE-2D) [10, 13] is developed in the frame of the KESS code by IKE institute at Stuttgart University and its models have been integrated in the German system code ATHLET-CD. The code describes the transient boil-off and quenching behaviors of debris bed, and thus can be applied to assess the coolability of particulate bed during severe accident in a light water reactor (LWR).

The MAWA code models the debris bed in two dimensions with cylindrical or Cartesian geometry using a quasi-continuum approach. Three separate phases, i.e. solid particles, liquid coolant (water) and gas (vapor), are considered. The solid particles are assumed to be a fixed matrix, while the fluid is treated as high-permeability porous medium (high porosity and large particle diameter) without separate model.

The MAWA code solves the basic two-phase conservation equations for mass, momentum and energy. Particularly, for the momentum equations, the temporal and spatial derivatives of the velocities can be neglected under two assumptions that the dominating forces on the fluids are particle-fluid and the interfacial drag, and that the response of the velocity field to the pressure variations is instantaneous, yielding a simplified equations as:

$$-\nabla p_g = \rho_g \vec{g} + \frac{\vec{F}_{pg}}{\varepsilon\alpha} + \frac{\vec{F}_i}{\varepsilon\alpha} \tag{1}$$

$$-\nabla p_l = \rho_l \vec{g} + \frac{\vec{F}_{pl}}{\varepsilon(1-\alpha)} - \frac{\vec{F}_i}{\varepsilon(1-\alpha)} \tag{2}$$

for vapor and liquid respectively. The friction force between the fluid and solid particles ($\vec{F}_{pg}$ and $\vec{F}_{pl}$) are modeled by using Ergun's equation [14] for one-phase flow, and extended for the two-phase flow by the introduction of relative permeability and relative passability:

$$\vec{F}_{pg} = \varepsilon\alpha \left(\frac{\mu_g}{K K_{rg}} \vec{j}_g + \frac{\rho_g}{\eta \eta_{rg}} |\vec{j}_g| \vec{j}_g \right) \tag{3}$$

$$\vec{F}_{pl} = \varepsilon(1-\alpha) \left(\frac{\mu_l}{K K_{rl}} \vec{j}_l + \frac{\rho_l}{\eta \eta_{rl}} |\vec{j}_l| \vec{j}_l \right) \tag{4}$$

For the interfacial drag, Schulenberg and Müller [15] proposed an equation based on the experiment data:

$$\vec{F}_i = 350(1-\alpha)^7 \alpha \frac{\rho_l K}{\eta\sigma} (\rho_l - \rho_g) g |\vec{j}_r| \vec{j}_r \tag{5}$$

where $\vec{j}_r$ is the relative velocity given by

$$\vec{j}_r = \frac{\vec{j}_g}{\alpha} - \frac{\vec{j}_l}{1-\alpha} \tag{6}$$

The capillary force in the form of pressure difference between vapor and pool ($p_c = p_g - p_l$) is also optionally considered in the momentum equation as a function of various parameters, including surface tension, contact angle, porosity and saturation. Several mostly used classic formulations for the frictional pressure drop of two-phase flow through porous medium are summarized in Table II.

In the simulation using MEWA code, since the geometry of the six test beds are all axial-symmetric, only half of the bed is considered as the computational domain and discretized into approximately 10^3 nodes.

For frictional model, only Reed model is used since Reed model is generally has a better agreement with the experiment data and is usually taken as a standard model with best adaptation [10, 16].

Table II. Formulations for the Friction Pressure Drop of Two-phase Flow through Porous Medium

Model	Parameters			
	p_c	K_r	η_r	F_i
Lipinski (1982)	$\frac{6\sigma(1-\varepsilon)cos\theta}{d\varepsilon}$	$K_{r,l}=s^3$ $K_{r,g}=\alpha^3$	$\eta_{r,l}=s^3$ $\eta_{r,g}=\alpha^3$	0
Reed (1982)		$K_{r,l}=s^3$ $K_{r,g}=\alpha^3$	$\eta_{r,l}=s^5$ $\eta_{r,g}=\alpha^5$	0
Hu and Theofanous (1991)	0	$K_{r,l}=s^3$ $K_{r,g}=\alpha^3$	$\eta_{r,l}=s^6$ $\eta_{r,g}=\alpha^6$	0
Schulenberg and Müller (1987)	0	$K_{r,l}=s^3$ $K_{r,g}=\alpha^3$	$\eta_{r,l}=s^5$ $\eta_{r,g}=\begin{cases}\alpha^6, \alpha>0.3\\ 0.1\alpha^4, \alpha\le 0.3\end{cases}$	$\vec{F}_i=350(1-\alpha)^7\alpha\frac{\rho_l K}{\eta\sigma}(\rho_l-\rho_g)g\lvert\vec{j}_r\rvert\vec{j}_r$

4. RESULTS AND DISCUSSIONS

4.1. MEWA Code Validation

The Comparison of the experimental data and results predicted by MEWA code is shown in Fig. 4, in which the numbers over the columns indicate the relative error. The y-axis quantity for all the test beds except Bed-4 (triangular) is dryout heat flux (kW/m^2), which is defined as the dryout power normalized by the cross-section area of the bed. While for Bed-4, the dryout power density (kW/m^3) is used instead to characterize the dryout power level since the cross section area varies along the height. It can be seen that the accuracy of the MEWA code predictions of the dryout power for various types of debris beds is overall satisfactory, with the maximum relative error within 16%. Therefore, generally speaking, MEWA code is applicable to predict the DHF for a particulate bed during severe accident scenario. However, it should also be noted that the MEWA predictions are somewhat overestimated compared to the experiment results.

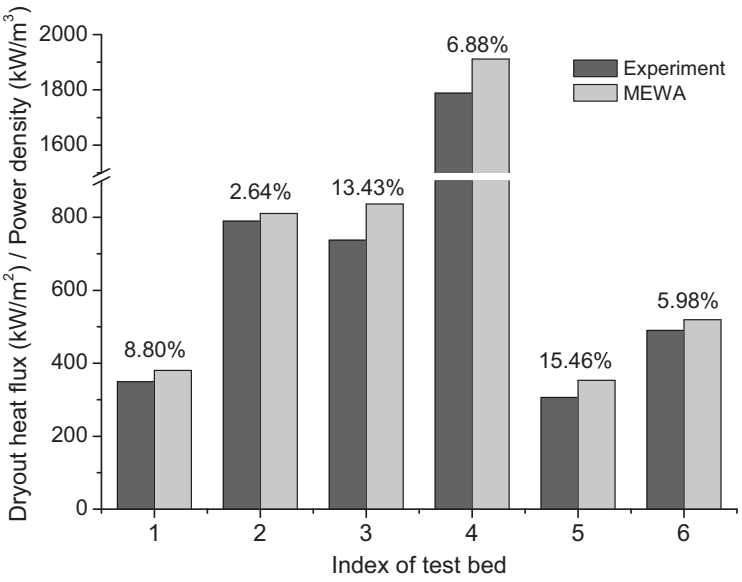

The y-axis quantity is dryout heat flux for all test Beds except Bed-4 (triangular), whose is dryout power density instead. The numbers above the columns are relative error.

Figure 4. Comparison of Experiment Data and MEWA Code Prediction

The dryout condition of the homogeneous bed, taking Bed-2 for example, is shown in Fig. 5. The liquid flood and quench the bed from the top while the vapor rise from the bottom in opposite direction. As the result, the dryout occurs near the bottom of the bed where the coolant has to penetrate the whole porous bed to reach, and the dryout heat flux is determined by CCFL. The predicted DHF of Bed-2 is roughly 2.2 times higher than Bed-1, which can be expected since the particle diameter and the porosity of Bed-2 are both larger, leading to a significant reduction of the frictional resistance [9].

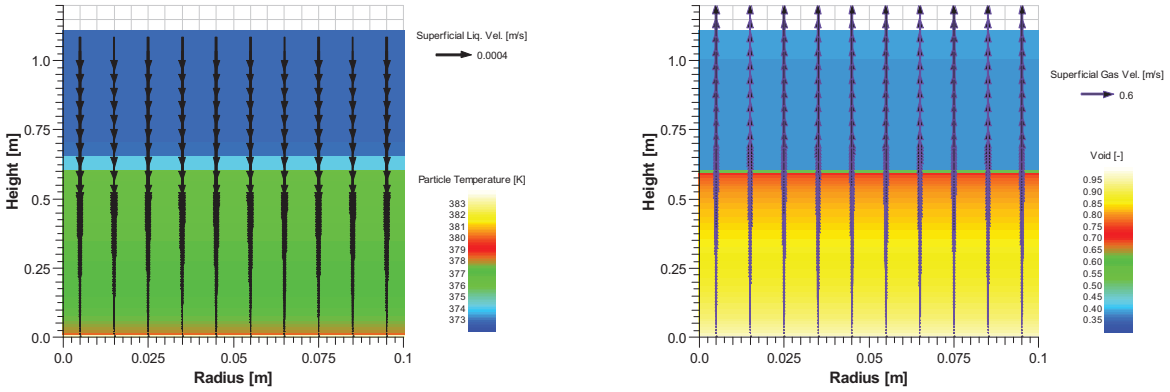

(a) Particle temperature and liquid velocity (b) void fraction and vapor velocity

Figure 5. Dryout Condition of the Homogeneous Bed (d=3.0mm)

Fig. 6 shows the particle temperature and vapor velocity of Bed-3 (radially stratified). The DHF of Bed-3 is comparable with the homogeneous Bed-2 packed with 3.0mm spheres, and much higher than the homogeneous Bed-1 filling with smaller diameter (1.5mm) spheres, which implies that the DHF of Bed-3 is dominated by the side column packed with larger size particles. This is because the side column

provides escape path for the vapor generated in the middle part due to the relatively smaller frictional resistance (Fig. 6b), resulting in more ingression of coolant from the top (Fig. 6a). Besides, the predicted location of dryout is in the upper part of the region with larger size particles, which also coincides with the observation of the experiment.

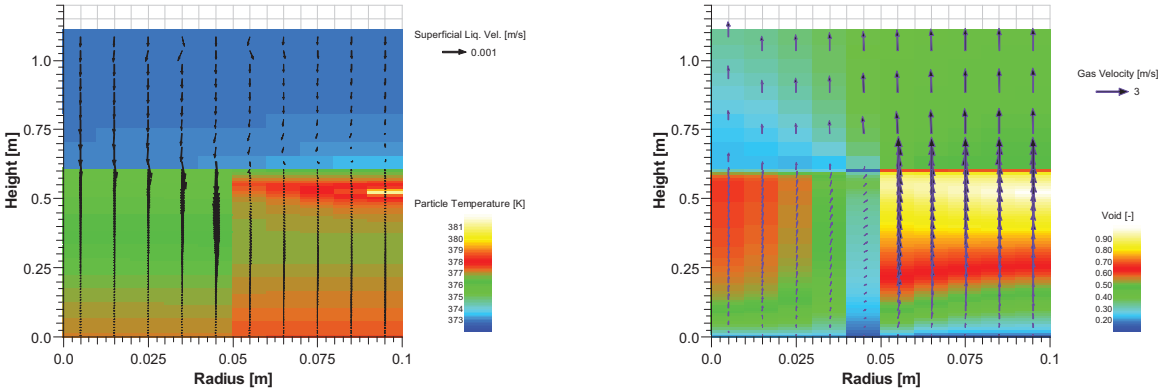

(a) Particle temperature and liquid velocity (b) void fraction and vapor velocity

Figure 6. Dryout Condition of Radially Stratified Bed-3

Fig. 7 shows the dryout condition of Bed-4 (triangular), from which it can be found that the dryout occurs in the inner and upper part of the triangular bed. Besides, the experiment also demonstrated that the dryout power density is much larger (69%) than a homogeneous bed which has a same volume, particle size and porosity with the triangular bed [11]. The reason is that the multidimensional packing fashion promotes the ingression of coolant from the sides and the bottom in addition to the top, so that the limitation of counter-current flow is removed which is favorable for the coolability.

As shown in Fig. 8, the dryout condition of Bed-5 (horizontally stratified) is similar to the homogeneous bed. In contrast to the radially stratified bed (Bed-3) whose DHF is dominated by the region with larger size spheres, the DHF of Bed-6 is much closer to that of the homogeneous bed with smaller size particles (Bed-2). The reason is that is the coolant floods from the top, while the region with larger size (3.0mm) particles is located beneath the region with smaller size (1.5mm) particles, which can't provide additional escape path for vapor to avoid CCFL.

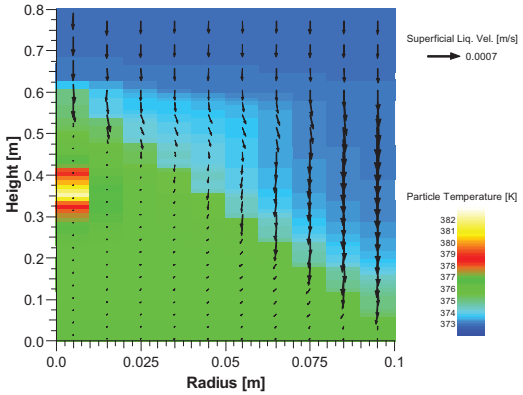

Figure 7. Particle temperature and liquid velocity of Triangular Bed-4

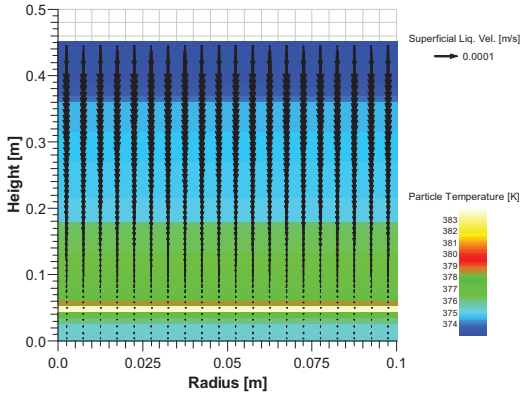

Figure 8. Particle temperature and liquid velocity of Horizontally Stratified Bed-5

Fig. 9 shows the dryout condition Bed-6 featuring multidimensional stratification. The location of dryout is predicted in zone4, the upper left region where particles with diameter of both 3.0mm and 1.5mm are mixed, which is consistent with the experiment observation. From Fig. 9 it is found that zone1~3 are accessible for coolant either from top or from side, while upward vapor accumulates in zone4 which prevent the ingression of coolant from top.

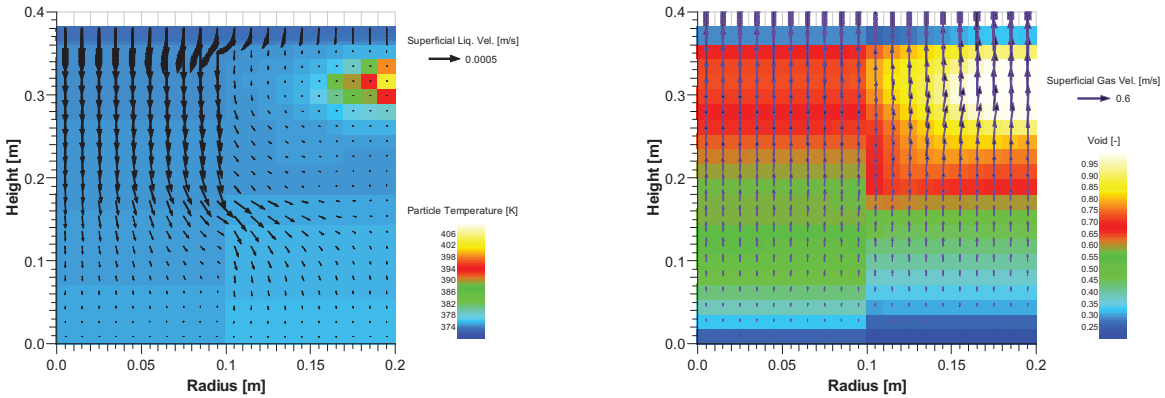

(a) Particle temperature and liquid velocity (b) void fraction and vapor velocity

Figure 9. Dryout Condition of Multi-Stratified Bed-6

4.2. Natural Circulation Driven Coolability

To investigate the so-called natural circulation driven coolability (NCDC), a downcomer is employed in POMECO-HT facility, though which the coolant from the top pool is accessible to the bottom of the debris bed and can flow upward driven by the buoyance. Two different sizes, 8mm and 12mm, of the inner diameter of the downcomer are applied in the experiment.

Fig. 10 shows the comparison of the MEWA predictions of DHF against experimental data for homogeneous bed packed with 1.5mm spheres (Bed-1) when the downcomer is considered, as well as the case without downcomer. The numbers above the columns are the relative error. It can be seen that generally the results predicted by MEWA match well with the experiment, and still somewhat overestimated. Moreover, compared to the top-flooding case without downcomer, the experimental dryout heat flux rises up to 19% with 8mm-ID downcomer and 34% using 12mm-ID downcomer, which indicates an evident enhancement of the coolability of the debris bed. This is because the downcomer provides natural circulation of the coolant from the bed bottom in addition to the top flooding, resulting in co-current flow of the vapor and liquid inside the bed (cf. Fig. 11). Therefore the limit of counter-current flow is broken, and the coolability is primary determined by the natural circulation flow rate instead.

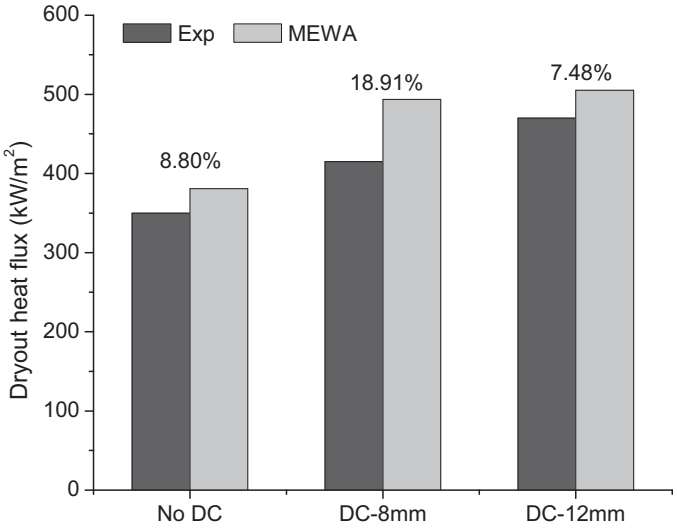

Figure 10. Dryout Heat Flux with Downcomer (Bed-1)

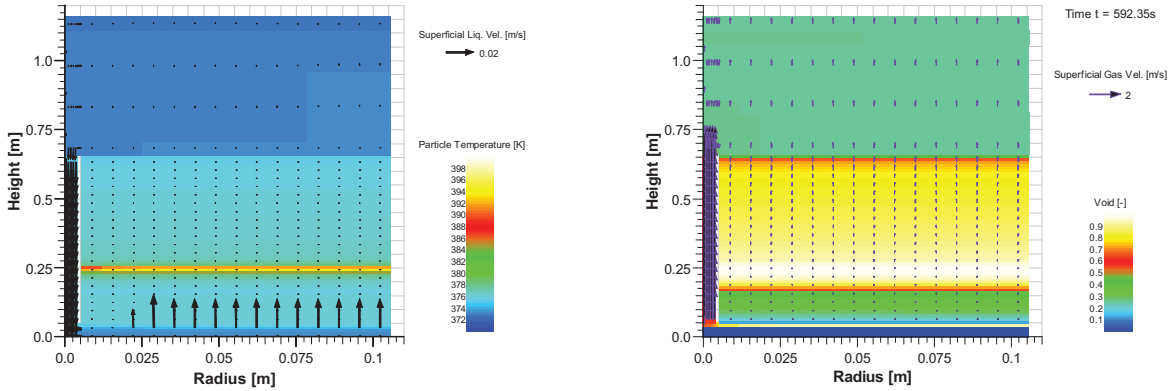

(a) Particle temperature and liquid velocity (b) void fraction and vapor velocity

Figure 11. Dryout Condition of Homogeneous Bed (d=1.5mm) considering downcomer

4.3. Interfacial Drag

The interfacial drag between the vapor and the liquid may affect the pressure field inside the debris bed, and further, the dryout heat flux. Schmidt [13] reported that the maximum coolable bed power increase remarkably if water access from below is enable, even only a minor fraction of the lower bound is directly connected to the coolant pool. Schäfer and Lohnert [17] found that the interfacial drag has an opposing effect on the coolability for different geometric configuration of the debris bed.

Among the commonly used models to predict pressure drop listed in Table II, only Schulenberg and Müller model takes account the interfacial dray in the momentum equation. To study the influence of the interfacial dray, two cases, i.e. top flooding and bottom injection, are considered in the present work. In the case of top flooding, the vapor and coolant flow reversely, while in the bottom injection case the vapor and coolant flow in the same direction. The interfacial drag is considered in the simulation by using Schulenberg and Müller model option in the MEWA code, and the injection of coolant from the bottom is modeled by assuming a hydrostatic pressure difference between the bottom and the top of the bed [10].

Fig. 12 depicts the dryout heat flux for both top-flooding and bottom-injection cases with and without the consideration of the interfacial drag. The pressure variation along the axial direction is shown in Fig. 13. Compared to the case without interfacial drag, the DHF slightly decreases (8.57%) for the top-flooding case, while significantly rises (63.89%) for the bottom-injection case when interfacial drag is included in the momentum equation. The reason is that for the top-flooding case, the vapor and liquid flow in the opposite direction. As the result, the inclusion of the interfacial drag increases the flow resistance, which hinders the escape of vapor and the ingression of coolant. The pressure at the bottom is reduced due to the growth of the frictional loss (Fig. 13a), which also contributes to the evaporation and thus the occurrence of dryout. For the bottom-injection case in which the vapor and liquid flow in the same direction, the interfacial dray helps to pull the coolant from the bottom. From Fig. 13b it can be seen that the pressure gradient is much larger when the interfacial drag is taken into account, which also can enhance the upward flow of the coolant.

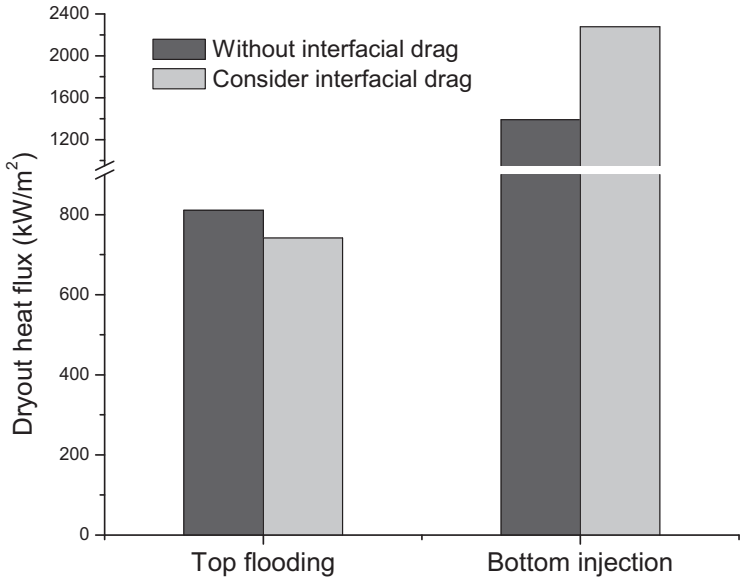

Figure 12. Comparison of DHF Regarding Interfacial Drag

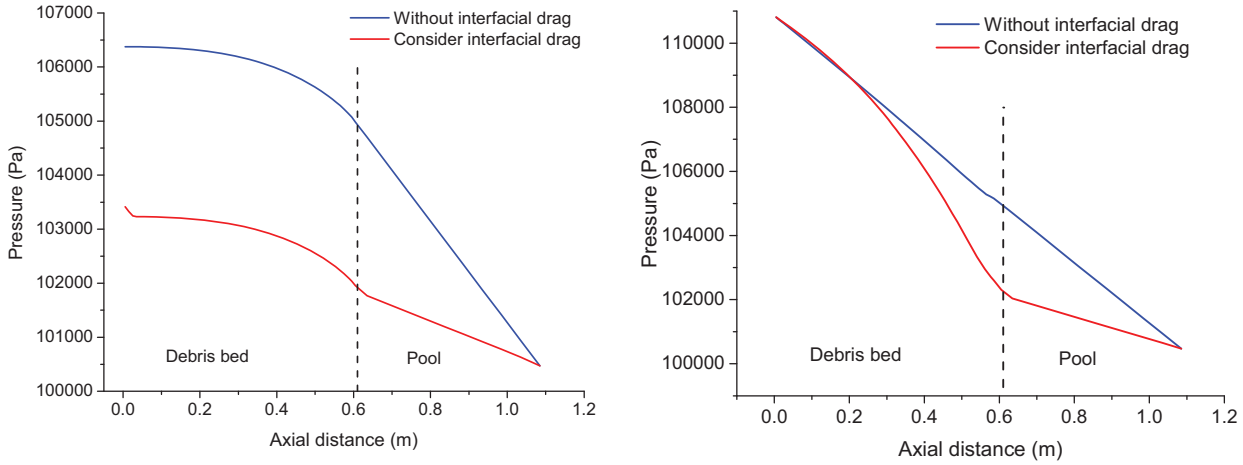

(a) top-flooding case (b) bottom-injection case

Figure 13. Pressure Profile along the Axial Direction

5. CONCLUSIONS

Aiming at validating the MEWA code for analyzing the coolability of particulate bed during severe accidents of light water reactors, the present work compares the results predicted by the code with the experimental data obtained from the POMECO-HT facility. Various configurations of the debris bed regarding the particles size and distribution are selected for validation, including homogeneous, radially stratified, triangular stratified, axial stratified, and multi-stratified debris beds. The results show that the MEWA code is applicable to predict the dryout condition for a debris bed during severe accident since the accuracy of prediction is satisfactory. However, it should also be noted that the MEWA calculation results are somewhat overestimated. For the 1-D top-flood case (e.g. homogeneous bed), the dryout heat flux mainly depends on counter-current flow limit. While for certain cases like radially stratification, the multidimensionality may help break CCFL by enhance the ingression of coolant from bottom or sides.

To investigate the effect of bottom-fed induced natural circulation, downcomers with different diameters are applied. The MEWA code calculating results match well compared to the experiment data. It is found that the coolability of debris bed can be enhanced when a downcomer is used due to the upward flow of coolant from the bottom that removes the counter-current flow limit.

The interfacial drag affects the coolability by means of varying the pressure field inside the bed. Its influence is studied by using the Schulenberg and Müller model option in the code instead of the commonly used Reed model. Both the top-flood and bottom-injection cases are considered, and the results show that the influence of interfacial drag differs. For the top-flood case, the dryout heat flux is slightly reduced since the interfacial drag increases the flow resistance due to the counter-current flow of vapor and coolant. The reducing pressure at the bottom due to the increase of the frictional loss also contributes to the occurrence of dryout. While for the bottom-fed case, the dryout heat flux rises remarkably when considering the interfacial drag, because the vapor and coolant flow in the same direction and the interfacial drag helps to pull coolant upward from the bottom. The pressure difference between the bottom and the top of the bed also enlarges by the interfacial drag, which can further enhance the upward flow of the coolant.

NOMENCLATURE

d	particle diameter (m)
F_{pg}	volumetric frictional drag force between solid particle and vapor (N/m^3)
F_{pl}	volumetric frictional drag force between solid particle and liquid (N/m^3)
F_i	volumetric interfacial drag force between solid vapor and vapor (N/m^3)
g	gravitational constant (m/s^2)
j	superficial velocity (m/s)
K	permeability (m^2)
K_r	relative permeability (-)
p	pressure (Pa)
$s = 1 - \alpha$	saturation (-)

Greek symbols

α	void fraction (-)
ε	porosity of debris bed (-)
η	passability (m)
η_r	relative passability (-)
θ	contact angle (rad)
μ	dynamic viscosity ($Pa \cdot s$)

ρ	density (kg/m^3)
σ	surface tension (N/m)

Subscripts

i	interface
l	liquid
g	gas, steam
r	relative
c	capillary force

REFERENCES

1. K. Hu and T.G. Theofanous, "On the Measurement and Mechanism of Dryout in Volumetrically Heated Coarse Particle Beds," *Int. J. Multiphase Flow*, **17**(4), pp. 519-532 (1991).
2. G. Hofmann, "On the Location and Mechanisms of Dryout in Top-Fed and Bottom-Fed Particulate Beds," *Nuclear Technology*, **65**, pp. 36-45 (1984).
3. S. Leininger, R. Kulenovic, et al., "Experimental Investigation on Reflooding of Debris Beds," *Annals of Nuclear Energy*, **74**, pp.42-49 (2014).
4. R.J. Liplnski, "A Model for Boiling and Dryout in Particle Beds," Report NUREG/CR-2646, SAND82-0765 (1982).
5. V. X. Tung and V. K. Dhir, "A Hydrodynamic Model for Two-Phase Flow through Porous Media," *Int. J. Multiphase Flow*, **14**(1), pp. 47-65 (1988).
6. A.W. Reed, "The Effect of Channeling on the Dryout of Heated Particulate Beds Immersed in a Liquid Pool," Ph.D. thesis, Massachusetts Institute of Technology, Cambridge (1982).
7. T. Schulenberg and U. Müller, "An Improved Model for Two-Phase Flow through Beds of Coarse Particles," *Int. J. Multiphase flow* **13**(1), pp. 87-97 (1987).
8. Eveliina Takasuo, Stefan Holmström, et al., "The COOLOCE Experiments Investigating the Dryout Power in debris beds of Heap-like and Cylindrical Geometries," *Nuclear Engineering and Design*, **250**, pp. 687-700 (2012).
9. Weimin Ma, Truc-Nam Dinh, "The Effects of Debris Bed's Prototypical Characteristics on Corium Coolability in a LWR Severe Accident," *Nuclear Engineering and Design*, **240**, pp. 598-608 (2010).
10. Manfred Bürger, Michael Buck, Werner Schmidt, et al., "Validation and Application of the WABE code: Investigations of Constitutive Laws and 2D Effects on Debris Coolability," *Nuclear Engineering and Design*, **236**, pp. 2164-2188 (2006).
11. Sachin Thakre, Liangxing Li, et al., "An Experimental Study on Coolability of a Particulate Bed with Radial Stratification or Triangular Shape," *Nuclear Engineering and Design*, **276**, pp. 54-63 (2014).
12. Sachin Thakre, Weimin Ma, "An experimental study on the coolability of stratified debris beds," *Proceeding of International Congress on Advances in Nuclear Power Plants (ICAPP)*, Charlotte, USA, April 6-9, pp. 1107-1112 (2014).
13. W. Schmidt, "Influence of Multidimensionality and Interfacial Friction on the Coolability of Fragmented Corium," Ph.D. Thesis, University of Stuttgart (2004).
14. S. Ergun, "Fluid Flow through Packed Columns," *Chem. Eng. Prog*, **48**(2), pp. 89-94 (1952).
15. T. Schulenberg and U. Müller,"A Refined Model for the Coolability of Core Debris with Flow Entry from the Bottom," *Proceedings of the Sixth Information Exchange Meeting on Debris Coolability*, University of California, Los Angeles, Vol. 18 (1986).
16. Liangxing Li, Weimin Ma, Sachin Thakre, "An Experimental Study on Pressure Drop and Dryout Heat Flux of Two-Phase Flow in Packed Beds of Multi-Sized and Irregular Particles," *Nuclear Engineering and Design*, **242**, pp. 369-378 (2012).
17. Patrick Schäfer, Günter Lohnert, "Boiling Experiments for the Validation of Dryout Models Used in Reactor Safety," *Nuclear Engineering and Design*, **236**, pp. 1511-1519 (2006).